

## Measurement and Evaluation of Earthing Parameters for Improved RSU Injection Substation Using Polynomial Technique

\*Dabotubo F. Harry<sup>1</sup>, Dikio C. Idoniboyeobu<sup>2</sup>, Sepribo L. Braide<sup>3</sup>,

<sup>1</sup>(Consulting Department of Dabochristy Electrical Services Nigerian LTD, Port Harcourt, Nigeria)

<sup>2&3</sup>(Department of Electrical Engineering, Rivers State University, Nigeria)

\*Corresponding Author: Dabotubo F.

**ABSTRACT:** This research work investigated the nature and safety compliance of the existing earthing system adopted in the 7.5MVA, 33/11KV Rivers State University (RSU) Estate/Works injection substation. Three-pin fall-of-potential method with Mastech MS2302 Digital Earth Resistance Tester was used to measure the earthing resistance and resistivity of the substation soil. Polynomial method was used to evaluate the measured earthing resistances whose results were validated with the standard Sunde and Dwight equations for a single and multiple earth rod resistances. The substation was upgraded from 11/0.415KV distribution station to 7.5MVA, 33/11KV injection substation in 2014. As new challenges emerge in power electrical workplace safety due to upgrade in injection substations, it is the responsibility of the system designer to seek out new approaches and solution that address them. The present 7.5MVA, 33/11KV injection substation has existing separate ground earthing arrangement with average resistance of 1.95 ohms. However, this fails to address the issue of surface potential distribution, since low earth resistance is not always a guarantee to safety. Ground grid earthing system arrangement is proposed to address this problem with reference to IEEE Std-80 approach. Electrical Transient Analyzer Program (ETAP) simulation environment was used to analyse the safety implementation and cost of the proposed ground grid model. Further study on earth potential rise and surface potential distribution with optimal compression ratio is recommended.

**Keywords** – Earthing; Earth Resistance and Resistivity; Polynomial equations; Ground Potential Rise; Ground Grid; Touch and Step Potentials; Mesh Potential; Fault Current.

Date of Submission: 27-04-2021

Date of acceptance: 11-05-2021

### I. INTRODUCTION

The study is based on earthing parameters measurement (Soil Resistivity and Resistance) using standard instrument, the measurements were evaluated with polynomial method and validated with Sunde and Dwight equations for single and multiple earth rod resistance calculation for improved RSU 7.5MVA, 33/11KV injection substation.

Improved earthing means, a better and more effective electrical connection to the general mass of the earth to provide safe passage of fault current to operate protective device as quick as possible and provide safety to personnel and equipment in the event of fault. The system of earthing adopted in power generation, transmission and distribution stations is of primary importance. Substation earthing system is essential not only to provide protection to human beings working within the vicinity of earthed facilities and equipment against electric shock but to also maintain proper, efficient and reliable functioning of the entire electrical network.

The topic on earthing system is often treated with levity to an extent in some electrical texts and literatures. This paper will present an improved step-by-step approach on earthing system design for 33/11KV substation and calculating necessary parameters for satisfactory performance, a case study on RSU Estate/Works 7.5MVA, 33/11KV injection substation Port Harcourt, Rivers State

### RELATED WORKS

An effective earthing system guarantees safe and reliable operation of substations. It ensures safety to personnel inside or in the immediate vicinity of the station. The earthing system provides low impedance path for fault current to earth without exceeding the operating limits of equipment. It ensures that in the event of

fault, the current is easily dissipated into the earth without exposing personnel on site to dangerous step and touch potential. Some related literatures for improving earthing system is discussed below.

Nevel (2014) in his work investigate the use of a high resistivity surface material (0.2m thick layer of river gravel) in improving the safety (step and touch voltages) while designing substation earthing grid in high soil resistivity area. Surface layer material becomes very important when designing a substation ground grid in high soil resistivity. A layer of crushed rock, chipping or gravel has become the design standard to provide a high resistance between the ground grid and personnel. If the underlying soil has a lower resistivity than the surface layer then only small amount of grid current flow into the surface layer resulting in small potential rise in the surface material hence low step and touch voltages. Though there must be a compromise with fault clearance time when considering surface material [14].

Lukong et al (2015) proposed a method for soil resistance reduction using biochar as soil enhancement material. In their investigation a cylindrical hole of 20cm in diameter and 1m deep was dug and the soil from this hole is replaced with biochar. Before the replacement water is sprinkled around the wall to ease contact with biochar and the native soil. This is preceded by compacting of the biochar into the hole. Analyzing the experimental results indicate a significant reduction in earth resistance with the application of biochar obtained from rice straw compared to the case without biochar treatment. Biochar is found to be rich in mineral salts with low resistance that can last as long as one hundred years from study. Biochar is cheap as its raw material (biomass), mostly waste is found almost everywhere in the world [11].

Buba S. D. et al (2016) studied the effect of earth rods on reduction of grid resistance using six different earth grid configurations. The two parameters considered were the spacing between grid conductors of compression ratio 1 and 0.8, and earth grid configuration installed with vertical rods and another without vertical rods at the grid periphery and last with vertical rods at all grid intersection. It was found that, grid designs with compression ratio of 0.8 yielded lower grid resistances than those with compression ratio of 1. Compression ratio of 1 means equally spaced rows and columns of parallel grid conductors, while a compression ratio of 0.8 represent closely spaced rows and columns of parallel conductors around the periphery and widely spaced towards the centre of grid. It was also revealed that reduction in the grid resistances obtained after installation of earth rods at all conductor intersections was negligible considering the increase in the total length of buried conductors. It was further discovered that the EPR produced by grids designed with compression ratio of 0.8 were lower than those with compression ratio of 1. They concluded that, installation of earth rods at all points of intersecting grid conductors with the aim of reducing the grid resistance is not recommended as the reduction in resistance of 0.11 ohm is not commensurate to the increase in buried conductor length of 1084 metres [3]

Ghoniem et al (2012) in their paper titled "Optimization of grounding grids design with evolutionary strategies" investigated the effect of adding vertical earth rods at different locations on Earth Surface Potential (ESP) study. This study describes how different grounding grid profile design with vertical rods can achieve convenient grid resistance, touch and step voltages with minimum cost. A 50x50m<sup>2</sup> grid with 4, 16, and 64 meshes, 0.005m radius grid rods, 2m vertical rods with 0.005m radius, 0.5m grid depth, homogenous soil resistivity of 2000 ohm-m are the grid characteristics. It is clear in their result that as the number of meshes increases, grid resistance, step and touch voltages decreased. It was further stated that a design of 16 meshes with 16 earth rods distributed equally around the perimeter can be selected as a good compromise between technical and economic aspects. It was observed that a change in locations of vertical rod resulted to a small reduction in ground potential rise (GPR). Hence, it is not convenient to use vertical rods with grounding grid buried in homogenous soil resistivity [6].

## II. METHODOLOGY

The study is based on earthing parameters measurement (Soil Resistivity and Resistance) using standard instrument, and evaluating such measurements amongst others with polynomial method and validating the polynomial method with Sunde and Dweight equations for single and multiple earth rod resistance calculation, with suggested improvement using the IEEE Std-80 for AC Substation design method.

### 3.2 Method Used

The IEEE Std-80 2013 (IEEE Guide for AC Substation design) method.

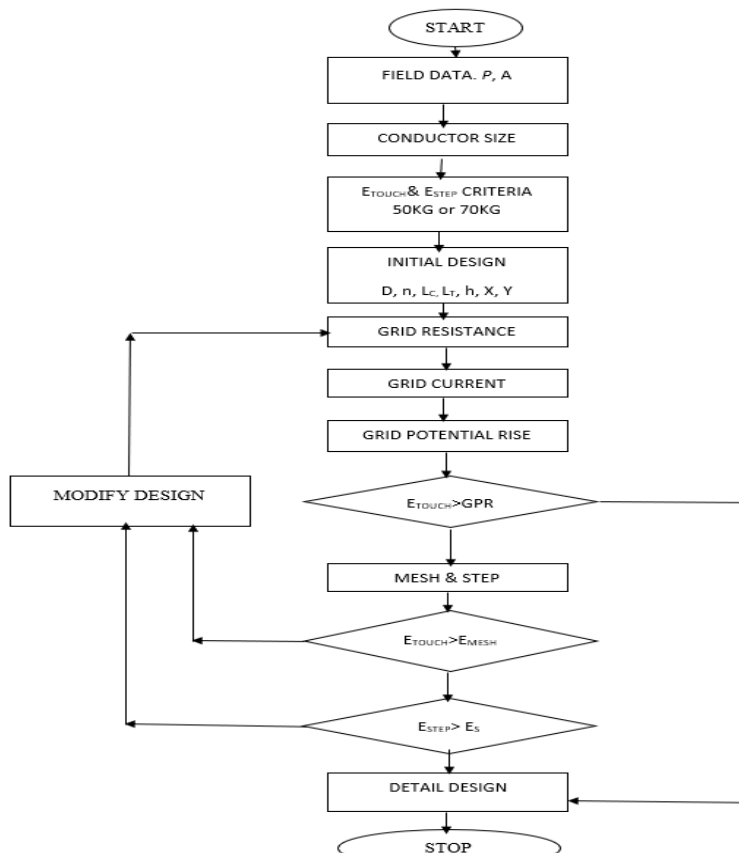


Figure 1: Earth Grid Design Work Flow Chart

3.2.1 Field Data (Soil Resistivity and Area of Earthen) (Step 1)

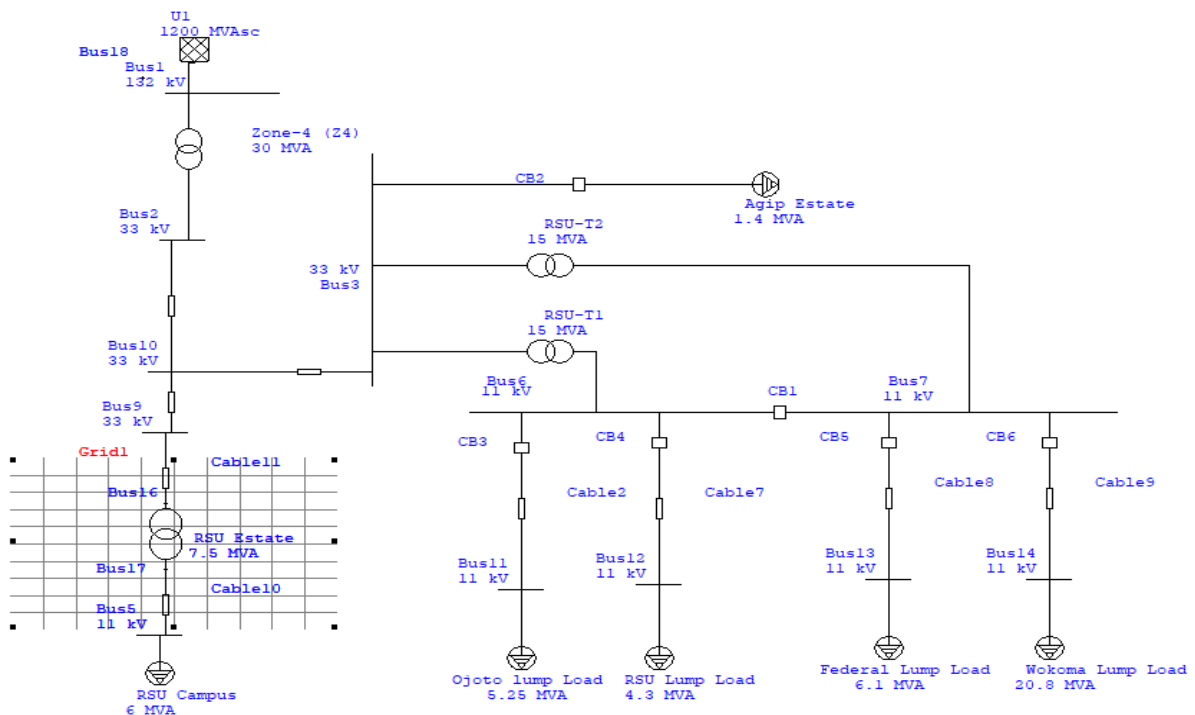


Figure 2: Network Diagram Showing the Ground Grid Area of Earthen

Note: Network diagram showing the ground grid area of earthen for the RSU 7.5 MVA Estate Injection Substation indicated as Grid-1 covering 528m<sup>2</sup>

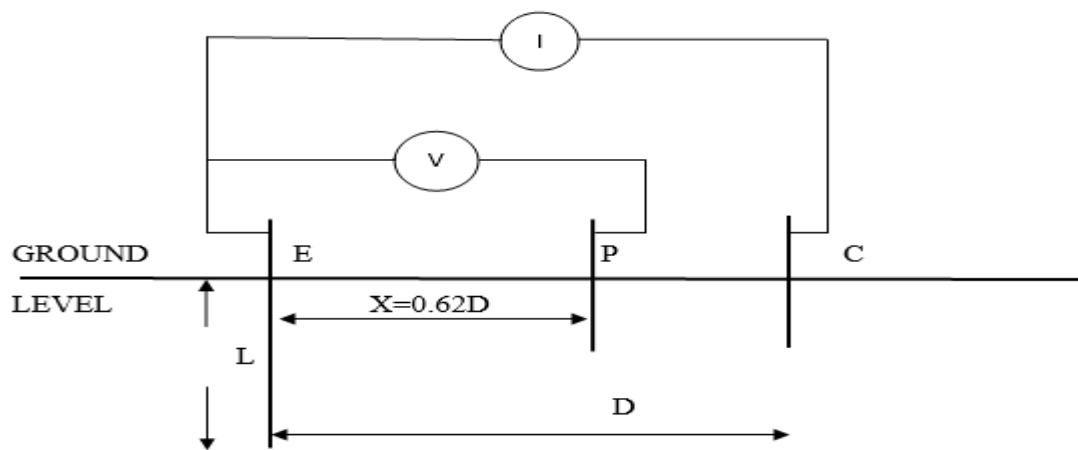


Figure 2: Fall-of-Potential or three pin driven rod method of resistivity test illustration

Table 1: Substation Soil Resistivity Test Results Using MS2302 Digital Earth Resistance Tester.

S/N	Length (L) of test rod (E) in metres	Auxiliary potential (P) electrode distance from test rod (E) in metres	Auxiliary current (C) distance from (E) in metres	Resistance measured in (ohms)	Resistivity in ohm-m
1	0.5	6.2	10	215	137.95
2	1.0	6.2	10	123	138.25
3	1.5	9.3	15	63.8	100.30
4	1.8	11.16	18	52.8	96.67
5	3.0	14.88	24	35.4	95.99

Note: The values of measured soil resistance and resistivity at different depth of test electrode while observing the 62% position of potential electrode is shown on column 5 and 6 of table 1.

Table 2: Effect of Change in Potential Electrode on Soil Resistivity

S/N	Length (L) of test rod E in metres	Different test position of potential electrode (P) in metres					Current electrode (C) distance from test rod E in metres
		1.0m	2.0m	3.2m	4.2m	5.3m	
1	1.5m	6.3m	7.8m	9.3m	10.8m	12.0m	15m
		12.5m	13.0m				
	Resistance in (ohms)	18.0	36.0	51.0	58.0	60.01	
		62.3	62.8	63.8	64.2	70.2	
		80.01	90.3				
	Resistivity in (ohm-m)	28.3	56.6	80.18	91.19	94.33	
		97.95	98.73	100.3	100.95	103.13	
	% of (P) electrode position from (E) of electrode (C)	6.6%	13.3%	21.3%	28%	35.3%	
		42%	52%	62%	72%	82%	
		83.3%	86.7%				

Note: Effect of change in potential electrode on soil resistivity and resistance values at different test positions of potential electrode is shown in rows 3 and 4 respectively of table 2, also the positions in terms of percentage of current electrode including the 62% position is given in the table.

3.2.1.1 Formulation of Polynomial Equation for Approximate Earthing Resistance Determination

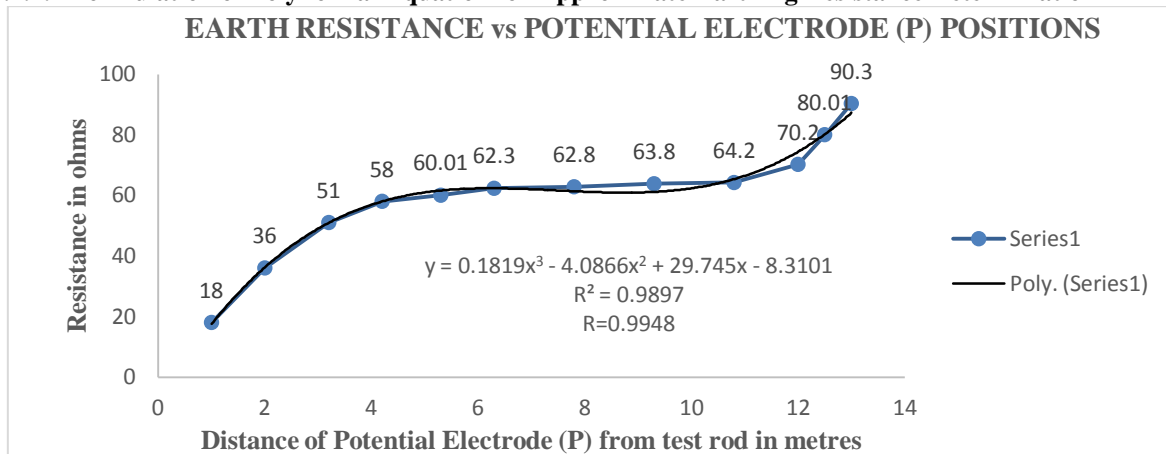


Figure 3: The Polynomial Equation Formulation

The polynomial equation describing the line of best fit in the plot of figure 3 from rows 2 and 3 measurement values of table 2 can be used to estimate the resistance value of an equivalent rod used for the measurement. Resistance value of different diameter can be evaluated with a factor  $D_{FH} = 1.08^{-n}$ ,  $n=0,1,2,3,4$  used to multiply the fundamental polynomial for every increase in diameter equal to the rod size used for the original plot in blue colour of figure 3, where  $n=0$  for the first measurement with a rod diameter of 0.01m.

$$y_n = \frac{1}{1.08^n} (0.1819x^3 - 4.0866x^2 + 29.745x - 8.3101), n = 0,1,2,3,4 \tag{1}$$

$$y_n = 1.08^{-n} (0.1819x^3 - 4.0866x^2 + 29.745x - 8.3101), n = 0,1,2,3,4, \tag{2}$$

$$y_0 = \frac{1}{1.08^0} (0.1819x^3 - 4.0866x^2 + 29.745x - 8.3101) \tag{3}$$

$$y_1 = \frac{1}{1.08^1} (0.1819x^3 - 4.0866x^2 + 29.745x - 8.3101) \tag{4}$$

$$y_2 = \frac{1}{1.08^2} (0.1819x^3 - 4.0866x^2 + 29.745x - 8.3101) \tag{5}$$

$$\frac{y_0}{y_1} = \frac{y_1}{y_2} = \frac{y_2}{y_3} = \frac{y_3}{y_4} = 1.08 \tag{6}$$

$$R_n = \frac{\rho a}{2\pi l_r} \left( \ln\left(\frac{8l_r}{d_r}\right) - 1 \right) \tag{7}$$

For more than one rod, the resistance can be approximated by equation 8, which closely compares with the standard Sunde and Dwight equation 10

$$y_{n_r} = \frac{1}{n_r} \left( y_n + \frac{32}{D} \gamma \right) \tag{8}$$

$$\text{where } \gamma = \sum_1^{n_r} \left( \frac{1}{n_r} \right) - 1 \tag{9}$$

$$R_{n_r} = \frac{\rho a}{2\pi n_r l_r} \left( \ln\left(\frac{8l_r}{d_r}\right) - 1 + \frac{l_r}{D} 2 \ln\left(\frac{1.781n_r}{2.718}\right) \right) \tag{10}$$

$n_r$  is the number of rods,  $D$  is the distance between two rods

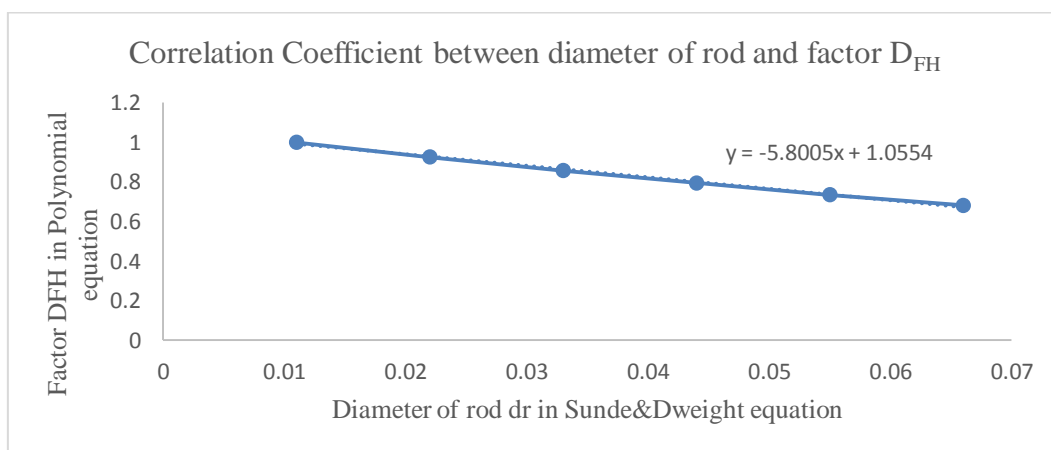


Figure 4: Plot of Correlation Coefficient between diameter of rod and polynomial variable factor  $D_{FH}$ .

The relationship between diameter of rod and polynomial variable factor  $D_{FH}$  within some specified linear region in the plot of figure 4 is given as equation 11.

$$D_{FH} = -5.8005d_r + 1.0554, \text{ for } 0.7 \leq D_{FH} \leq 1 \quad (11)$$

Where  $D_{FH}$  is the polynomial coefficient determining factor

### 3.2.2 Conductor Size (Step 2)

$$A_{mm^2} \geq \frac{\sqrt{I^2 t_f}}{K} \quad (12)$$

$$K = \sqrt{\frac{TCAP \times 10^{-4}}{\alpha_T \times \rho_T} \times \ln \left[ \left( \frac{K_G + T_m}{K_G + T_a} \right) \right]} \quad (13)$$

The value of  $K$  can be calculated from the material constants given in table 1[8].

Substitution of operating temperature of 49°C into equation 13 gives a  $K$  value of 0.04

### 3.2.3 Step and Touch Voltage Criteria (Step 3)

The choice of body weights between 50kg and 70kg in calculating touch and step voltages actually depend on the expected weight of personnel at the site. Control of human body weight into the substation would be practically difficult, hence a conservative choice of 50kg body weight is chosen for the purpose of this research work. For a crushed rock with resistivity  $\rho_s$  of 4267.2 ohm-m with thickness  $h_s = 0.1402m$  and fault clearance time of 0.5 seconds, the tolerable touch and step voltages is given as:

$$V_{Touch,50kg} = (1000 + 1.5 \times 0.7655 \times 4267.2) \frac{0.116}{\sqrt{0.5}} = 967.87 \text{ volts} \quad (14)$$

$$V_{Step,50kg} = (1000 + 6 \times 0.7655 \times 4267.2) \frac{0.116}{\sqrt{0.5}} = 3,379.28 \text{ volts} \quad (15)$$

$$C_s = 1 - \frac{1 - \frac{\rho_1}{\rho_s}}{1 + 22.22h_s} = 1 - \frac{1 - 154/4267.2}{1 + 22.22 \times 0.1402} = 0.7655 \quad (16)$$

### 3.2.4 Initial Mesh and Step Potential Parameters Calculations (Step 4)

$$D_x = \frac{L}{n_x - 1} \quad (17)$$

$$D_y = \frac{W}{n_y - 1} \quad (18)$$

$$L = 24m, W = 22m$$

For  $D_x = 12$ , and  $D_y = 11$  we have  $n_x = 3$  and  $n_y = 3$ . Thus, we have a grid system of 3x3 with average conductor spacing given as;

$$D_a = \frac{D_x + D_y}{2} = 11.5 \quad (19)$$

### 3.2.4 Ground Grid Resistance Calculation (Step 5)

Schwarz equations considered a grid with earth rods modeled separately as parallel resistances with mutual effect between grid and earth rod resistances in a two-layer soil model. These equations as found in IEEE Std-80 and given below:

$$R_g = \frac{R_c R_r - R_m^2}{R_c + R_r - 2R_m} \quad (20)$$

$$R_c = \frac{\rho_1}{\pi L_c} \left[ \ln \left( \frac{2L_c}{a} \right) + \frac{K_1 L_c}{\sqrt{A}} - K_2 \right] \quad (21)$$

$$R_r = \frac{\rho_{av}}{2\pi n_r L_r} \left[ \ln \left( \frac{8L_r}{d_r} \right) - 1 + \frac{2K_1 L_r}{\sqrt{A}} (\sqrt{n_r} - 1)^2 \right] \quad (22)$$

$$R_m = \frac{\rho_{av}}{\pi L_c} \left[ \ln \left( \frac{2L_c}{L_r} \right) + \frac{K_1 L_c}{\sqrt{A}} - K_2 + 1 \right] \quad (23)$$

$$\rho_{av} = \frac{l_r (\rho_1 \times \rho_2)}{[\rho_2(H-h) + \rho_1(l_r + h - H)]} \quad (24)$$

$R_c$  is ground resistance of grid conductors in ohms

$R_r$  is ground resistance of all grid rods in ohms

$R_m$  is mutual resistance between group of grid conductors,  $R_c$ , and of ground rods,  $R_r$  in ohms

$\rho_{av}$  is the apparent resistivity seen by the ground rods and mutual resistances.

$\rho_1 = 154 \Omega m$ ,  $\rho_2 = 100 \Omega m$ ,  $L_r = 5.49 m$ ,  $L_c = 138 m$ ,  $H = 1.5 m$ ,  $h = 0.8 m$ ,  $A = 528mm^2$

### 3.2.5 Grid Current (Step 6)

From the short circuit study of the network of figure 2 above, a maximum of 5.0kA three phase to ground short circuit current at bus-5 located in the secondary side of the substation was achieved

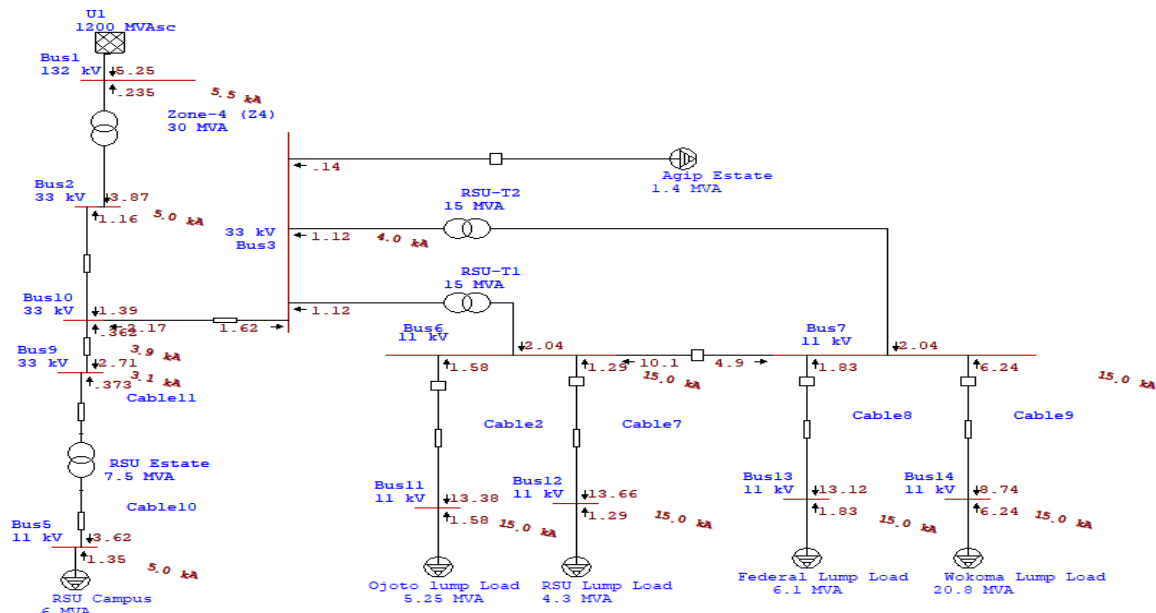


Figure 5: Short Circuit current value at bus-5 in the study is 5KA

**3.2.6 Grid Potential Rise (GPR) (Step 7)**

The equation for the ground potential rise is given as;

$$GPR = R_g \times I_g \times S_f \tag{25}$$

$$GPR = 1.7908 \times 5,119 \times 1 = 9168.11 \text{ Volts}$$

$S_f$  is the current split factor

**3.2.7  $E_{TOUCH} > GPR$  (Step 8)**

Ground Potential Rise (GPR) is greater than tolerable touch potential, hence corner mesh and step potential will be calculated for safety check for the proposed grid design in the next step-9.

**3.2.8 Corner Mesh ( $E_m$ ) and Step ( $E_s$ ) Potentials (Step 9)**

$$E_m = \frac{\rho \times I_g \times K_m \times K_i}{L_C + L_R \left[ 1.55 + 1.22 \left( \frac{L_r}{L_x^2 + L_y^2} \right) \right]} \tag{26}$$

$$K_m = \frac{1}{2\pi} \left\{ \ln \left[ \frac{D^2}{16hd} + \frac{(D+2h)^2}{8Dd} - \frac{h}{4d} \right] + \frac{K_{ii}}{K_h} * \ln \left[ \frac{8}{\pi(2n-1)} \right] \right\} \tag{27}$$

$$E_s = \frac{\rho \times I_g \times K_s \times K_i}{0.75L_C + 0.85L_R} \tag{28}$$

$$K_s = \frac{1}{\pi} \left[ \frac{1}{2 \times h} + \frac{1}{D+h} + \frac{1(1-0.5^{n-2})}{D} \right] \tag{29}$$

**3.2.9  $E_{TOUCH} > E_m$  (Step 10)**

From the above calculations it is clear that tolerable touch voltage of equation 16 is greater than the corner mesh voltage of equation 40, hence we proceed to the next step-11.

**3.10  $E_{STEP} > E_s$  (Step-11)**

Similarly, the calculated value of tolerable step voltage is greater than the corner step voltage, thus we proceeded to implementing the detail design in step-13 using ETAP 16.0

**III. RESULTS AND DISCUSSIONS**

Table 3 shows comparison between Sunde & Dwight equation 8 and Polynomial equation 1 for a single earth electrode resistance for different values of diameter of the test rod and the results tabulated in columns 5 and 6 for Sunde & Dwight and Polynomial equation respectively. Between the extremes of the polynomial variable factor  $D_{FH}$ , other special critical values of diameter (dr) exist that separate different quantitative resistances for the solution behaviour. The accuracy of the predictive polynomial equation outside the defined range of the  $D_{FH}$  factor in equation 11 is very slim, thus, (+3.8%) of calculated values obtained must be added for diameter values less than or equal to 0.011.

**Table 3: Comparison Between Actual Earth Resistance Value and Polynomial Result At 62% (X=9.3) Of Potential Electrode (P) For Single Rod**

S/N	$l_r$ (m)	$d_r$ Diameter of rod	Resistivity $\rho_a$ in $\Omega$ -m	$R_n$ $\Omega$	$(y_n)$ (x=9.3m)	$R_n - y_n$	%error	C(x)
1	1.5	0.011	100	63.6	61.2	2.4	3.8%	15m
2	1.5	0.022	100	56.25	56.65	-0.4	0.71%	15m
3	1.5	0.033	100	51.95	52.45	-0.5	0.96%	15m
4	1.5	0.044	100	48.9	48.58	0.32	0.65%	15m

Table 4 shows comparison between total resistance of Sunde & Dwight equation 10 and polynomial equation 8 for 4 rods ( $n_r = 4$ ), and calculated results corresponding to these values for different diameter of rod are tabulated in columns 5 and 6 respectively. The difference in these results in decimal values and percentages are also tabulated in columns 7 and 8. A resistivity of 100 ohm-m was used in the calculation, different values of resistivity in percentage of 100 can be used, (example, 80 ohm-m resistivity value correspond to 0.8 which will multiply the polynomial equation for a predictive result).

**Table 4: Comparison Between Polynomial Equation 8 And Sunde & Dwight Equation 10 For 4 Rods**

S/N	$l_r$ (m)	$d_r$	Resistivity $\rho_a$ in $\Omega$ -m	$R_{n_r}$ $\Omega$ ( $n_r = 4$ )	$(y_{n_r})$ ( $n_r = 4$ )	$R_{n_r} - y_{n_r}$	%error	C(x)
1	1.5	0.011	100	18.46	18.19	0.27	1.46%	15m
2	1.5	0.022	100	16.62	17.05	-0.43	2.59%	15m
3	1.5	0.033	100	15.54	16.00	-0.46	2.96%	15m
4	1.5	0.044	100	14.78	15.03	-0.25	1.69%	15m

**Table 5: Ground Grid Simulation Result from ETAP 16.0**

Project: Mtech Project	ETAP	Page: 1
Location: Rivers State University	16.0.0C	Date: 02-20-2020
Contract: PG2018/00476		SN: 4359168
Engineer: Dabotubo F. Harry	Study Case: RSU Estate	Filename: Dabo

**Ground Grid Summary Report**

Rg Ground Resistance ohm	GPR Ground Potential Rise Volts	Touch Potential			Step Potential		
		Tolerable Volts	Calculated Volts	%	Tolerable Volts	Calculated Volts	%
1.791	9170.7	967.9	925.9	95.7	3379.4	409.4	12.1
Total Fault Current:		5.000 kA		Reflection Factor (K):	-0.930		
Maximum Grid Current:		5.119 kA		Surface Layer Derating Factor (Cs):	0.766		
				Decrement Factor (Df):	1.024		

Note: The above results in table 5 is from ETAP 16.0 simulation from ground grid input parameters of appendix 1.

**IV. CONCLUSION**

Measurement and evaluation are an integral part of substation earthing consideration. Therefore, it must be designed to be reliable and cost efficient. Substations are critical part of the electrical network usually manned by human beings on daily basis hence it must have improved surface potential distribution which occur in separate grounding during fault current and lightning surges for adequate protection of lives. The design must provide good earth grid in the substation in an economic and technically viable manner for regular upgrade.

The measurement value of the earthing properties was evaluated/implemented into Sunde/Dwight equations which are validated by the formulated predictive polynomial equations/model.

APPENDIX

Appendix 1: Input Parameters for Ground Grid Simulation

Constants IEE							
Code	Kim	Kis	Km	Ks	Kii	K1	K2
A	1.08821	1.08821	1.033136	0.2386757	1	1.367048	5.622239

Ground Soil Input Data									
Code	MaterialType0	Resistivity0	Depth0	MaterialType1	Resistivity1	Depth1	MaterialType2	Resistivity2	
A	Crushed rock	4267.2	0.14	Moist soil	154	1.5	Moist soil	100	

Ground Grid Input Data

System Data:

Freq. Hz	Weight kg	Ambient Temp. °C	Short-Circuit Current			Fault Duration (Seconds)			
			Total Fault Current kA	Sf Division Factor %	Cp Projection Factor %	Tf for Total Fault Duration	Tc for Sizing Ground Conductors	Ts for Available Body Current	
50.0	50	40.00	5.000	7.58	100.0	100.0	0.50	0.50	0.50

Soil Data:

Surface Material			Upper Layer Soil			Lower Layer Soil	
Material Type	Resistivity Ohm.m	Depth m	Material Type	Resistivity Ohm.m	Depth m	MaterialType	Resistivity Ohm.m
Crushed rock	4267.2	0.140	Moist soil	154.0	1.50	Moist soil	100.0

Material Constants:

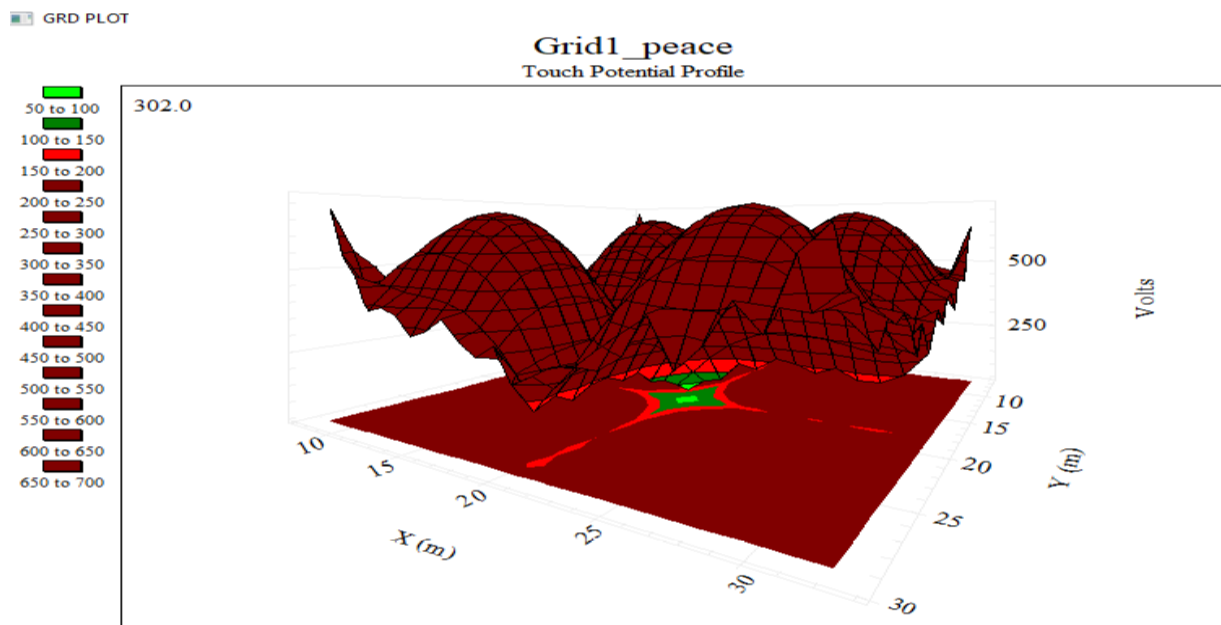
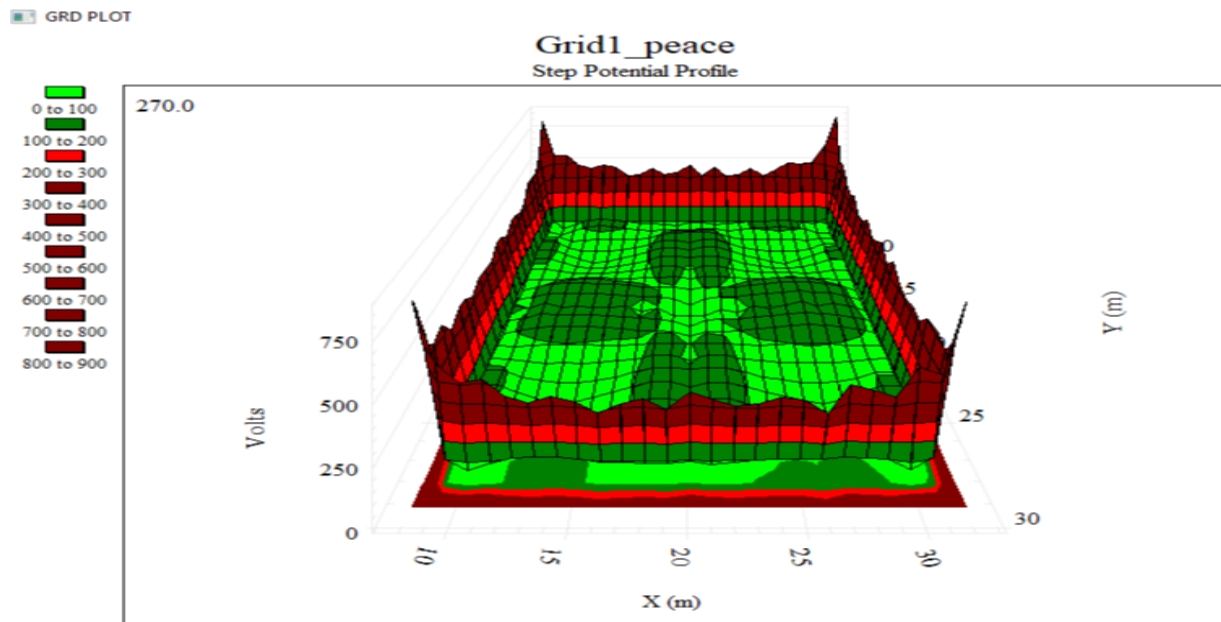
Conductor/Rod	Type	Conductivity %	$\alpha$ r Factor @ 20 °C 1/°C	K0 @ 0 °C	Fusing Temperatur °C	Resistivity of Ground Conducto @ 20°C e	Thermal Capacity Per Unit J/(cm <sup>3</sup> .°C) micro ohm.cm/Volume
Conductor	Copper, commercial hard-drawn	97.0	0.00381	242.0	1084.0	1.78	3.42
Rod	Copper-clad steel rod	20.0	0.00378	245.0	1084.0	8.62	3.85

Rod Data:

Diameter cm	Length m	No. of Rods	Arrangement	Cost \$/Rod
3.810	5.49	85	Rods Throughout Grid Area	13.00

Conductor Size mm <sup>2</sup>	Depth m	Grid Length m Lx Ly	Number of Conductors in X Direction	Number of Conductors in Y Direction	Separation m in X Direction	Separation m in Y Direction	Cost \$/m	Shape
95	0.80	24.00 22.00	3	3	12.0	11.0	10.00	Rectangular

## Appendix 2: Surface Potential Distribution Study Results for Step and Touch Voltages of The Proposed Ground Grid Using Finite Element Method (FEM) In ETAP 16.0



### REFERENCES

- [1]. Andrew, A., Sen, P. K. & Clifton, O. (2014). Designing safe and reliable grounding in AC substations with poor soil resistivity: An interpretation of IEEE Std. 80, 1-7.
- [2]. BS 7430 (2011). Code of Practice for Protective Earthing of Electrical Installations.
- [3]. Buba, S. D., Wan Ahmad, W. F., Ab Kadir, M. Z. A., Gomes, C., Jasni, J., & Osman, M. (2014). Reduction of Earth Grid Resistance by addition of Earth Rods to various Grid Configurations. ARPN Journal of Engineering and Applied Science. 11(3), 4533-4538.
- [4]. Esobinenwo, C. S., Akinwole, B. O. H., & Omeje C. O. (2014). Earth mat design for 132/33kv substation in Rivers state using ETAP. International Journal of Engineering Trends and Technology (IJETT). 15(8), 389-402.
- [5]. Ghoneim, S. S. M & Kamel, A. S. (2013). Analytical Method for Earth Surface Potential Calculation for Grounding Grids. International Journal of Engineering and Computer Science. 13(3), 47-53.
- [6]. Ghoneim, S., Hirsch, H., Elmorshedy, A. & Amer, R. (2007). Optimization of grounding grid design with evolutionary strategies. IEEE General meeting, Tempa, Florida, USA. 2007. 36-58.
- [7]. Hellany, A., Nagrial, M., Nassereddine, M., & Rizk, J. (2011). Safety compliance of substation earthing design. World academy of science, engineering and technology. 5(12), 341-345.

- [8]. IEEE Std 80 (2013). IEEE Guide for safety in AC substation grounding.
- [9]. Jinliang, H., Rong, Z., & Bo, Z. (2013). Methodology and Technology for Power System Grounding.
- [10]. Yexu Li & Dawalibi, F. (2012). Advanced Practical Considerations of Fault Current Analysis in Power System Grounding Design, Journal of International Council on Electrical Engineering, 2(4), 409-414,
- [11]. Lukong, P. N., Noel, D., Lenzemo, W. V., & Fagbenro, J. A. (2015). An Efficient Method for Electrical Earth Resistance Reduction Using Biochar. International Journal of Energy and Power Engineering. 4(2), 65-70.
- [12]. Muhammad, A. A. (2014). Improvement of substation earthing. International Journal of Engineering and Advanced Technology (IJEAT) 2014. 3(4),100-104.
- [13]. Nassereddine, M., Hellany, A., & Rizk, J. (2009). How to Design an effective Earthing System to ensure the safety of people. International Conference on Advances in Computer Tools for Engineering Apparatus 2009, 416-421.
- [14]. Nevil, J. (2014). Design of earth grid for 33/11kv GIS substation at a high soil resistivity site using CYMGRD software. International Journal of Engineering Research and Technology, (IJERT). 3(10), 1151-1155.
- [15]. Okereafor, F. C., Idoniboyeobu, D. C., & Bala, T. K. (2017). Analysis of 33/11KV RSU Injection Substation for Improved Performance with Distributed Generation (DG) Units. American Journal of Engineering Research (IJER). 6(9), 301-316.
- [16]. Okyere, P. Y. & George, E. (2006). Reducing Earth Electrode Resistance by Replacing soil in Critical Resistance Area. International Journal of modern Engineering. 6(2), pp. 2-9.
- [17]. Ossama, G., Ghada, A. & Hana I. (2011). Earth Surface Potential and GPR of Substation Grounding. 21st International conference on Electricity Distribution, Frankfurt, June 6-9. Paper No. 0020, 1-6.
- [18]. Paul, G. (2009). Electrical Power System Grounding and Resistance Measurement in Electrical Power Equipment Maintenance and Testing. 2nd ed, Boca Raton, FL CRC Press. 710-713.
- [19]. Rao, S.S. (2008). Switchgear Protection and Power Systems.13th edition, Khanna Publishers, New Delhi India, 2007.
- [20]. Roy, B.C. & Joseph, A. (2007). Designing for a Low Resistance Earth Interface Grounding. A publication of Lightning Eliminators & Consultants, Inc.USA,1-15.
- [21]. Thomas & Betts (2014). A guide to BS EN 62305 Protection Against Lightening
- [22]. Uma, U.U., Uzoechi, L.A., & Robert, B.J. (2016). Optimization Design of Ground grid Mesh of 132/33KV Substation using ETAP. Nigerian Journal of Technology. 35(4), 926-934.

Dabotubo F, et. al. "Measurement and Evaluation of Earthing Parameters for Improved RSU Injection Substation Using Polynomial Technique." *American Journal of Engineering Research (AJER)*, vol. 10(5), 2021, pp. 65-75.